



# A Deep Insight of Spermatogenesis and Hormone Levels of Aqua-Cultured Turbot (*Scophthalmus maximus*)

Yifan Liu<sup>1,2,3,4</sup>, Qinghua Liu<sup>2,4\*</sup>, Shihong Xu<sup>2,3,4</sup>, Yanfeng Wang<sup>2,3,4</sup>, Chengcheng Feng<sup>2,3,4</sup>, Chunyan Zhao<sup>2,3,4</sup>, Zongcheng Song<sup>5</sup> and Jun Li<sup>2,3,4\*</sup>

## OPEN ACCESS

### Edited by:

Yngvar Olsen,  
Norwegian University of Science  
and Technology, Norway

### Reviewed by:

Yichao Ren,  
Qingdao Agricultural University, China  
Ian A. E. Butts,  
Technical University of Denmark,  
Denmark

### \*Correspondence:

Jun Li  
junli@qdio.ac.cn  
Qinghua Liu  
qinghualiu@qdio.ac.cn

### Specialty section:

This article was submitted to  
Marine Fisheries, Aquaculture  
and Living Resources,  
a section of the journal  
Frontiers in Marine Science

**Received:** 21 August 2020

**Accepted:** 14 December 2020

**Published:** 11 January 2021

### Citation:

Liu Y, Liu Q, Xu S, Wang Y,  
Feng C, Zhao C, Song Z and Li J  
(2021) A Deep Insight  
of Spermatogenesis and Hormone  
Levels of Aqua-Cultured Turbot  
(*Scophthalmus maximus*).  
Front. Mar. Sci. 7:592880.  
doi: 10.3389/fmars.2020.592880

<sup>1</sup> National Engineering Research Center for Marine Aquaculture, Zhejiang Ocean University, Zhoushan, China, <sup>2</sup> The Key Laboratory of Experimental Marine Biology, Centre for Ocean Mega-Science, Institute of Oceanology, Chinese Academy of Sciences, Qingdao, China, <sup>3</sup> Southern Marine Science and Engineering Guangdong Laboratory, Guangzhou, China, <sup>4</sup> Laboratory for Marine Biology and Biotechnology, Qingdao National Laboratory for Marine Science and Technology, Qingdao, China, <sup>5</sup> Weihai Shenghang Aquatic Product Science and Technology Co. Ltd., Weihai, China

Turbot (*Scophthalmus maximus*) is an important marine fish both in Europe and North China. Although there are plenty of studies on the reproduction of turbot, the complete cytological process of spermatogenesis remains unclear. In this study, we investigated the submicroscopic structure of total 23 types of male germ cells throughout the breeding season, with a relatively complete process of the primary spermatocytes. We found that the spermatid tail formed early at Spermatid II, and there were at least 16 spherical mitochondria in the spermatozoa. The hepatosomatic index (HSI) and gonadosomatic index (GSI) both peaked during the breeding season. Preliminary analysis showed that the vitality of mature sperm was negatively correlated with the proportion of sperm deformity. The serum 3,5,3'-triiodothyronine (T3), 5-hydroxytryptamine (5-HT), testosterone (T), 17 $\alpha$ ,20 $\beta$ -Dihydroxy-4-pregnen-3-one (17 $\alpha$ ,20 $\beta$ -DHP), and 17 $\beta$ -estradiol (E2) all increased during the maturity period, with the change of T content most noticeable. Whereas in the testis, an overall high level of 11-ketotestosterone (11-KT) was more remarkable. The expression and localization of androgen receptor (*AR*) mRNA showed that the *AR* was highly expressed at the stages of II (15 – 70 g), with a slight rebound at the mature stages [IV(2200 g) to V(2500 g)], whose change was ahead to the changes of T and 11-KT. Fluorescence *in situ* hybridization (FISH) analysis showed that the *AR* mainly distributed in but not limited to Sertoli cells. This study represents the most complete overview of the reproductive cycle and spermatogenesis of turbot, which provides an important reference for the reproduction research and the guidance of flatfish breeding.

**Keywords:** fish reproduction, spermatogenesis, factory farmed fish, steroids, *Scophthalmus maximus*

## INTRODUCTION

Spermatogenesis is a highly complex and precise process, during which spermatogonia undergo proliferation and differentiation (mitosis and meiosis), developing to spermatocytes and then spermatids, and finally mature into spermatozoa. Errors in any step would cause the reduction of sperm quality and quantity. Reproductive maturity is considered to be final oocyte maturation and ovulation in females and the spermiation in males, and thereafter, their exact ratio in spawning events (Mylonas et al., 2010; Palma et al., 2019). For aqua-cultured fishes, especially those require artificial insemination, the gametes always come from specific broodstock group. The quality of sperm has gradually gained attention because it affects the health status even early life history of the offspring (Kroll et al., 2013; Siddique et al., 2017; Benini et al., 2018).

Although great numbers of literature on fish spermatogenesis are available, few studies systematically describe the entire cytological process of spermatogenesis in marine fish. The existing researches mainly focus on the general process of spermatogenesis or spermiogenesis in Nile tilapia (*Oreochromis niloticus*) (Lou and Takahashi, 1989), zebrafish (*Danio rerio*) (Leal et al., 2009; Rupik et al., 2011), silver pomfret (*Pampus argenteus*) (Chung et al., 2010), and stone flounder (*Kareius bicoloratus*) (Kang et al., 2016). The relative scarcity of these basic data may be due to the difficulties in sample collection during continuous and detailed developmental stages, and the difficulties in simultaneously capturing various types of germ cells in a small number of images. Besides, it is harder to differentiate the spermatogonial generations among the different stages of meiosis and spermiogenesis (Leal et al., 2009), which is largely due to the lack of a unified classification standard. Therefore, to systematically display the detailed process of spermatogenesis, continuous sampling and a large number of microscopic images are required.

In contrast, there are more reports of hormones during fish reproduction, including studies on sex steroids (e.g., androgen, estrogen, and progesterone) (Weltzien et al., 2002; Miura et al., 2006; Schulz et al., 2008, 2010; Björn et al., 2013; Chen et al., 2013; Hachero-Cruzado et al., 2013; O'Shaughnessy, 2014; Chauvigné et al., 2016, 2017; Hyeon et al., 2019), and other hormones [e.g., thyroid, and 5-hydroxytryptamine (5-HT)] (Bertil, 1994; Fallah-Rad et al., 2001; Holsberger et al., 2005; Mendis-Handagama and Siril Ariyaratne, 2005; Kreke and Dietrich, 2008; Wagner et al., 2008; Munakata and Kobayashi, 2010), which all involved in the spermatogenesis and the maintenance of male function. These works have provided us with ideal candidates in studying the regulation of steroid hormones during spermatogenesis.

Turbot (*Scophthalmus maximus*) is a demersal fish native to sandy shallow waters throughout the Mediterranean, the Baltic Sea, the Black Sea, and the North Atlantic. Nowadays, it has become an important aqua-cultured flatfish with a high economic value both in Europe and China (FAO, 2005). It was first introduced to north China in 1992 and has undergone nearly 20 years of factory farming (Lei, 2003, 2005; Song et al., 2019). The aquaculture industry of turbot has become very mature, which is

now the most successful model for aquaculture breeding in China (Gui et al., 2018).

Up to date, there are plenty of studies on turbot reproduction. The origin and migration of primordial germ cells were investigated through *in vivo* visualization by using genetic markers, including *vasa*, *dnd* (Lin et al., 2012, 2013), and *nanos3* (Zhou et al., 2019). The germ cells and early gonadal development during sex differentiation were examined by using histological sections (Zhao et al., 2017). The characteristic of progesterin and its receptors during the annual reproductive cycle of male turbot were studied (Feng et al., 2018). The function of vitamin E in stimulating the expression of gonadotropin hormones in the pituitary *in vitro* was reported (Huang et al., 2019). DNAJC19 and Sox2 were identified to participate in sexual development and reproduction by comparative mapping from linkage groups (Hermida et al., 2013). Transcriptomic study were also carried out to investigate the gonadal sex differentiation (Ribas et al., 2017) and spermatogenesis (Wang et al., 2018). All of these works have well described the biological characteristics of turbot reproduction. However, like most marine fishes, the cytological process of spermatogenesis in turbot remains to be systematically elucidated.

Moreover, in China, cultured turbot broodstock cannot naturally release gametes or fertilize (Lei and Men, 2002; Zhao et al., 2018; Song et al., 2019). The grasp of the sperm maturity period is largely dependent on the experience of the farmworkers, and the artificially extruded semen is usually in poor quality and shows sperm deformity, which compromises the health condition of the offspring (Lei and Men, 2002). Therefore, it is particularly important to grasp the timing of sperm production, which requires a thorough understanding of spermatogenesis.

This study aimed to investigate the complete cytological development process of the male germ cells, and reveal the changes of hormones throughout the reproductive cycle of turbot. We devoted particular attention to its major developmental events and the period-specific hormones in spermatogenesis. These data will provide crucial references for the reproduction study of both turbot and other flatfishes. Moreover, the results will also help to improve the guidance on broodstock breeding and gamete production of turbot.

## MATERIALS AND METHODS

### Fish Stocks

Juvenile and adult turbots were cultivated in a commercial fish farm (Shangdong Oriental Ocean Sci-Tech Co., Ltd.). The fish were kept in the 10 m × 10 m cement farming pond, with the flowing water system to maintain the quality of the seawater. The juveniles were less than 2 years old, whose ages were from 6 to 22 months ( $15.62 \pm 2.13$  g –  $1001.40 \pm 57.79$  g), with the ambient temperature kept between  $16 \pm 0.5$  and  $18 \pm 0.5^\circ\text{C}$ , on a 12L: 12D photoperiod. The broodstock were over 2 years old ( $1962.80 \pm 418.28$  g –  $2995.33 \pm 159.86$  g), and the rearing temperature was stable at  $16 \pm 0.5^\circ\text{C}$  during breeding season, with photoperiod management in the order of 8L: 16D (about 1.5 months), 12L: 12D (about 0.6 months) and 16L:

8D (about 4 months, approximately from the beginning of the seasonal gonadal development to 2.5 months after the end of the reproductive cycle) to regulate gonad development. Other rearing conditions were as follows: salinity  $31 \pm 0.5$ , dissolved oxygen  $> 7.0$  mgL<sup>-1</sup>, pH 7.6 – 8.1, feeding twice a day with enhanced nutrition (small yellow croaker *Larimichthys polyactis*, Pacific sand lance *Ammodytes personatus*, and cuttlefish).

We randomly collected 104 male turbot throughout the breeding season, with 6–8 individuals at each developmental stage. The male juveniles were sampled at 6, 10, 12, 14, 16, 20, and 22 months, and the male adults were collected from February to September. We checked the developmental stages of the very testis by paraffin section and found the testes are from stage II to stage VI (**Supplementary Figure 1**).

Before sampled, anesthetized 6–8 fish by using MS-222 (tricaine methanesulfonate; Sigma, United States). Then measured every individual and recorded the total weight, body weight, length, liver weight, and gonad weight. The hepatosomatic index (HSI, %) was calculated as liver weight  $\times 100$ /body weight, while the gonadosomatic index (GSI, %) was calculated as gonad weight  $\times 100$ /body weight. For each fish, the blood was collected from the caudal vein using disposable syringes (see “Hormones immunoassay”). Dissection after blood collection, then divided the left testis for histological analysis [paraffin sections, TEM, and SEM, see section “Transmission and scanning electron microscopy (TEM and SEM) assay”] and divided the right testis for further molecular research [q-PCR and FISH, see section “Quantitative Real-Time PCR (qRT-PCR) and Fluorescence *in situ* Hybridization (FISH)”]. Before the specific assay, used paraffin sections to check the actual development stages of each testis and group them.

## Transmission and Scanning Electron Microscopy (TEM and SEM) Assay

Randomly selected six of the sampled fish at each developmental stage for the TEM and SEM assay. For transmission electron microscopy (TEM), cut the geometric center of the left part of each testis into fragments ( $< 1$  mm) and immersed them by 2.5% glutaraldehyde in  $1 \times$  phosphate buffered saline ( $1 \times$  PBS) (pH 7.3). After fixation over 4 h at 4°C, the tissues were washed with  $1 \times$  PBS for three times (10 min each) and post-fixed by 2% osmium tetroxide (OsO<sub>4</sub>) in 1PBS over 4 h at 4°C. Then the tissues were washed repeatedly in distilled water and dehydrated by using a graded ethanol series (30, 50, 75, 95, 100, and 100%) for 10–20 min each. The samples were then embedded in Epon-Araldite and kept in dark at 4°C. Used a Reichert Ultracut E ultramicrotome to cut the samples into Semi-thin sections (1.5  $\mu$ m). Then stained the sections with 5% methylene blue (1 min, room temperature) before washed with  $1 \times$  PBS for three times (5 min each). Thereafter, use a Nikon Ni-E light microscope with a Nikon DS-Ri2 imaging system to find the target area. Then cut the samples into ultrathin sections (75–80 nm) by using the Ultracut E ultramicrotome, stained them with uranyl-less EM stain, and counterstained them with lead citrate. Finally, photographed the sections by using a transmission electron microscope Hitachi H-7000 5 (Hitachi, Tokyo, Japan).

For scanning electron microscopy (SEM), the dehydrated samples were transferred into propylene oxide, air-dried, and coated with gold-palladium. Then the samples were observed and photographed by using JEOL JSM-840A (JEOL, Tokyo, Japan).

## Sperm Analysis

Randomly selected nine samples of semen for further analysis. Use the Sperm Class Analyzer (Microptic, Barcelona, Spain) to analyze Sperm motility and curvilinear velocities (VCL). The results showed that the motilities were between 40 and 90%. An aliquot of 1  $\mu$ L semen was activated with 100  $\mu$ L seawater (pH 7.1) containing 0.1% bovine serum albumin (BSA). Sperm motility was defined as the percentage of moving spermatozoa with a VCL  $> 45$   $\mu$ m/s at 15 s after sperm activation (Feng et al., 2018). The sperm deformity ratio of each sample was calculated by TEM images.

## Hormones Immunoassay

Collected the blood of six fish at each developmental stage from the caudal vein by using disposable syringes (1, 5, and 10 mL; Xinhua, Shanghai, China) and clot at 4°C for 6–12 h. Then separated the serum by centrifugation at 4°C and 8,000 g for 10 min before analysis. Half a piece of testis was ground and homogenized in  $1 \times$  PBS by a 1: 9 mass-volume dilution ratios. After centrifugation at 4°C and 12,000 g for 10 min, the supernatant was sucked for the test. The levels of 3,5,3' triiodothyronine (T3), 5-hydroxytryptamine (5-HT), testosterone (T), 11-ketotestosterone (11-KT), 17 $\alpha$ , 20 $\beta$ -dihydroxy-4-pregnen-3-one (DHP) (17 $\alpha$ ,20 $\beta$ -DHP), progesterone (P4), 17 $\beta$ -estradiol (E2) and estriol (E3) were measured with radioimmunoassay (RIA) and enzyme-linked immunosorbent assay (ELISA) by Union Medical & Pharmaceutical Technology (Tianjin, China). The concentration of T3 was measured using Iodine [<sup>125</sup>I]. Radioimmunoassay Kits (Tianjin Nine Tripods Medical & Bioengineering Co., Ltd., Sino-US joint-venture enterprise) according to the manufacturer's protocol, with a highly specific binding rate (cross reactivity  $< 0.1\%$ ). The serum 5-HT was measured using ELISA kits (Diagnostic Systems Laboratories Inc., United States) according to the manufacturer's protocol. The T, 11-KT, 17 $\alpha$ ,20 $\beta$ -DHP, P4, E2, and E3 levels in the serum and the testis were measured by using the radioimmunoassay Kit (Tianjin Nine Tripods Medical & Bioengineering Co., Ltd., Sino-US joint-venture enterprise) according to the manufacturer's protocols, with highly specific binding rates respectively (cross reactivity  $< 0.1\%$ ).

## Quantitative Real-Time PCR (qRT-PCR) and Fluorescence *in situ* Hybridization (FISH)

Randomly selected six of the sampled fish at each developmental stage for the molecular study. Extracted the total RNA from the right part of each testis by using the Fastagene RNAfast 200 kit (Fastagen, China), and then checked the quantity and quality. The cDNA was synthesized by using the PrimeScribe RT reagent kit (Takara Bio, China) following the manufacturer's

instructions. Fluorescent real-time PCR was analyzed by using SYBR Premix real-time PCR kit with a Bio-RAD<sup>®</sup> CFX connect system. The PCR reactions were performed in triplicate with a 20  $\mu$ L reaction volume containing 10  $\mu$ L Top Green qPCR Super Mix (TransStart, China), 0.4  $\mu$ L Passive Reference Dye I, 1  $\mu$ L forward and reverse primer mix, 1  $\mu$ L template cDNA, and 7.6  $\mu$ L H<sub>2</sub>O. After incubation for 1 min at 95°C, the reaction was continued for 40 cycles at 95°C for 5 s and 60°C for 30 s. The reference genes *ubq* and *rsp4* and the target genes *AR* were amplified by using genespecific primers (Table 1), and the main qRT-PCR parameters were E% 1.01–1.04 and R<sup>2</sup> 0.996–0.999.

The samples used for FISH were collected from geometric center of the left part of each testis ( $n = 6$ ). They were fixed in 4% paraformaldehyde (1  $\times$  PBS, pH 7.2, 4°C). After fixation over 6 h at 4°C, the testes were dehydrated in a series of sucrose and embedded in O. C. T. Compound (Tissue-Tek, United States). Then the testes were cut into sections (5–8  $\mu$ m). Sense and antisense *AR* and *Sox9* probes were synthesized by using the DIG RNA Labeling Kit (Roche, Germany), and the primers used for FISH were listed in Table 1.

The sections were hybridized with the sense/antisense probes (65°C, 12 h), then incubated with horseradish peroxidase (POD)-conjugated anti-FITC-antibody (Roche, Germany) by a 1: 2000 dilution in the blocking solution to detect the FITC signal (4°C, overnight). After washed in 1  $\times$  PBST for three times, the samples were incubated for 1 h in TSA-Fluorescein by a 1: 150 dilution in TSA Amplification Buffer. The samples were then incubated with POD-conjugated anti-DIG antibody (Roche) by a 1: 1000 dilution in blocking buffer with 1% H<sub>2</sub>O<sub>2</sub> (4°C, overnight). After washed in 1  $\times$  PBST for three times, the samples were incubated in TSA-Plus Tetramethylrhodamine (1 h). Double color fluorescence *in situ* hybridization was performed using tyramide signal amplification TSA<sup>TM</sup> Plus Fluorescein & Tetramethylrhodamine (TMR) (PerkinElmer, United States). The nuclei were stained by using 4'-6-Diamidino-2-phenylindole (DAPI) and embedded with ProLong<sup>®</sup> Gold Anti-fade reagent (Invitrogen, Thermo Fisher, United States). Finally, the samples were observed and photographed by using a Nikon Eclipse 50i fluorescence microscope (Nikon, Tokyo, Japan).

## Statistical Analysis

Statistical analysis was carried out by using Statistics Package for Social Science (SPSS 21.0, SPSS Inc., United States), with the data expressed as means  $\pm$  standard error of mean. Data among groups were compared by one-way analysis of variance (ANOVA) followed by Duncan's multiple range tests. The Mantel-Haenszel  $\chi^2$  statistic was used to test for the association between Sperm motility and sperm deformity ratio.  $P < 0.05$  was considered statistically significant.

## RESULTS

### Hepatosomatic and Gonadosomatic Indices

To simulate the reproductive season under industrialized culturing conditions, we used specific photoperiods to induce

the development of the testis. Figure 1 showed the total length and weight of the fish at the stages from II to VI, including six different weight periods at stage II (15.62  $\pm$  2.13, 25.65  $\pm$  5.69, 69.68  $\pm$  14.19, 232.40  $\pm$  27.25, 414.67  $\pm$  58.40, and 823.25  $\pm$  40.43 g), two at stage III (1001.40  $\pm$  57.79 and 1962.80  $\pm$  418.28 g), one at stage IV (2179.75  $\pm$  273.47 g), one at stage V (2471.50  $\pm$  384.50 g), and three at stage VI (2545.00  $\pm$  512.88, 2566.67  $\pm$  39.75, and 2995.33  $\pm$  159.86 g). Grouped the fish by histological stages and approximate total weight as follows: II(15 g), II(25 g), II(70 g), II(240 g), II(400 g), II(800 g), III(1000 g), III(2000 g), IV(2200 g), V(2500 g), VI(2500 g), VI+(2500 g), and VI++(2900 g).

The trends of hepatosomatic index (HSI) and gonadosomatic index (GSI) were similar (Figure 2), both of which peaked during the breeding season ( $p < 0.05$ ). However, at the stage of VI++(2900 g), the GSI increased slowly, while the HSI continuously decreased.

### Cytological Process of Spermatogenesis

The TEM assay of the testes from different gonadal stages showed various types of male germ cells, including five types of spermatogonia (Figure 3A), ten types of spermatocytes (Figure 3B), seven developmental stages of spermatids, and the mature spermatozoa (Figure 3C). The major changes of morphology, cell diameters and nuclear diameters were listed in Table 2, with the entire process of spermatogenesis showed in Figure 4.

The Adiff (8 cell) were found to be in the anaphase of mitosis, whose nuclear membrane was disappeared and 2 sister chromatids were separated, pulled by the spindle fiber, and moved to the poles of the cell (Figure 3Ac). Besides, the B Late in the anaphase of mitosis was observed (Figure 3Ae).

Primary spermatocytes included eight different stages of primary spermatocytes, nearly covered the complete phases of meiosis I (Figures 3Ba–h). The duration of each developmental stage of primary spermatocytes was predicted based on its frequency, and it displayed as follows: Prophase I Pachytene > Prophase I Leptotene > Prophase I Zygotene > Prophase I Diplotene > Metaphase I > Anaphase/Telophase I > Prophase I Diakinesis.

It is worth mentioning that the distribution of the secondary spermatocytes, especially those at the stage of Post Telophase II (which would soon transform to Spermatid I) in the spermatocyst, was further dispersed, although they were still physically linked (e.g., by cytoplasmic bridges, Figure 3Bk). Moreover, compared to the primary spermatocytes, the distribution of the secondary spermatocytes was closer to the spermatids-rich area, although they were still separated by certain boundaries.

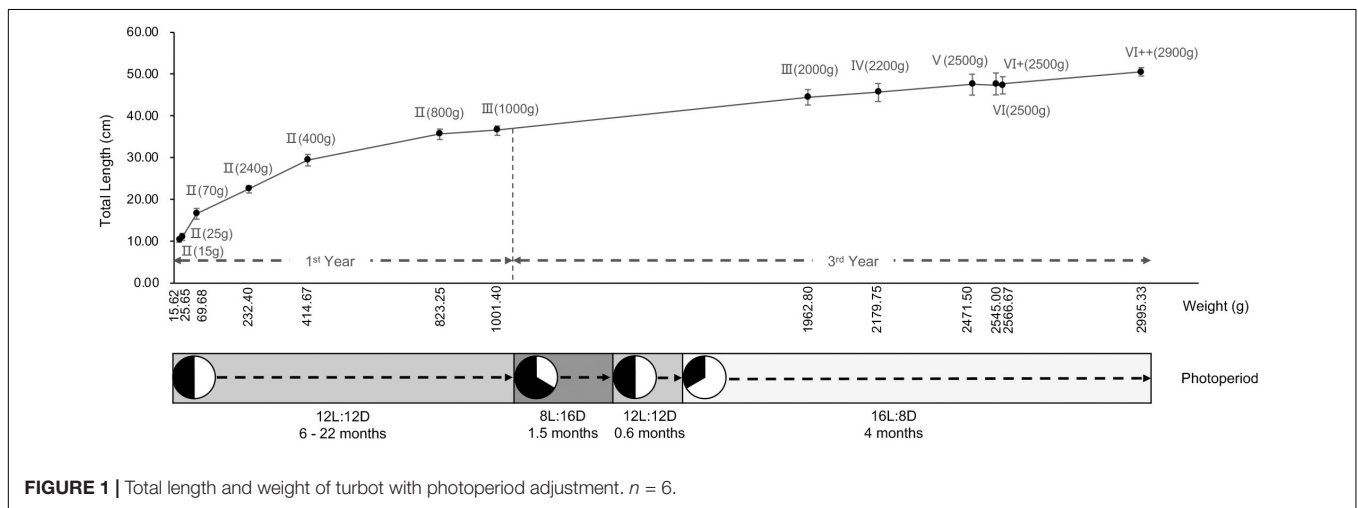
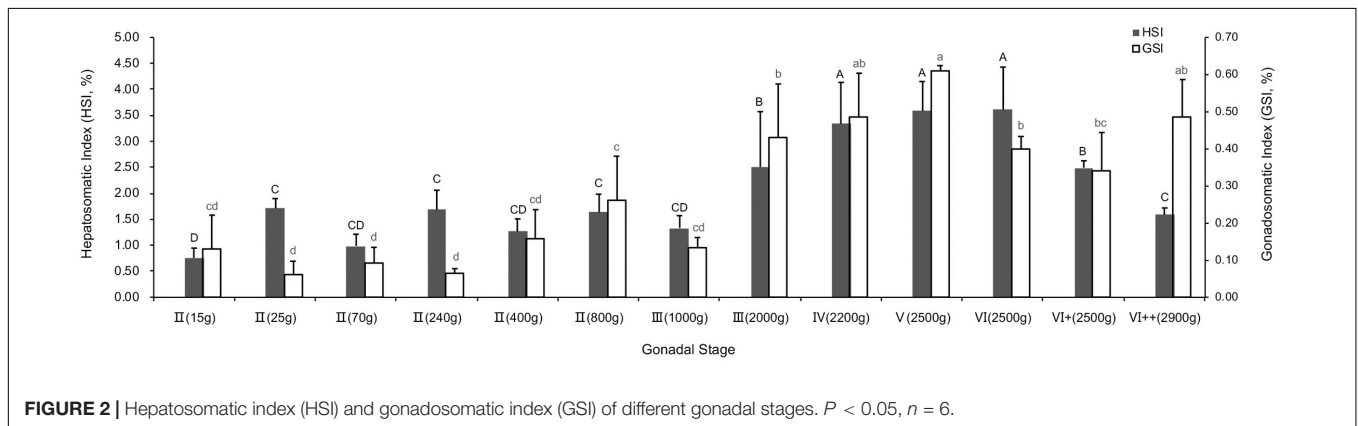
The spermiogenesis was divided into 8 different stages according to the typical morphological characteristics. The SEM results of the cell sizes was in agree with the TEM results (Figure 3Ci).

### Sperm Deformity and Sperm Motility

Compared with the normal sperm (Figures 5Aa,b) (Zhang et al., 2013), the SEM results in Figures 5Ac–f showed multiple

**TABLE 1** | Primer sequences used for qRT-PCR and FISH.

Primer name	Primer Sequence (5' to 3')	Product Length	Accession ID	Purpose
<i>Ubc-F</i>	GCGTGGTGGCATCATTGAGC	124	FE946708	qRT-PCR
<i>Ubc-R</i>	CTTCTTCTTGGGCAGTTGACAG			
<i>Rsp4-F</i>	CAACATCTTCGTCATCGGCAAGG	143	FE943956	
<i>Rsp4-R</i>	ATTGAACCAGCCTCAGTGTTAGC			
<i>AR-F</i>	CCATTACGGGGCACTCACC	160	KR019997	
<i>AR-R</i>	AGCTTCGAAACACCTCCTCAG			
<i>AR-FISH-F</i>	ATGTTCCCTATGGAGTTCTTCTTTC	511		FISH
<i>AR-FISH-R</i>	GCCCACCTTGACCACCTTTGAC			
<i>Sox9-FISH-F</i>	GACTTTGGAGCCGTGGACAT	666	KY677741	
<i>Sox9-FISH-R</i>	TCACGGTCTGGACAGTTGTG			

**FIGURE 1** | Total length and weight of turbot with photoperiod adjustment.  $n = 6$ .**FIGURE 2** | Hepatosomatic index (HSI) and gonadosomatic index (GSI) of different gonadal stages.  $P < 0.05$ ,  $n = 6$ .

sperm deformities, including the abnormalities of the head and mitochondria. Nine samples of semen were then randomly selected and their motilities were between 40 and 90%. As the sperm motility increased, the sperm deformity ratio reduced steadily from 36.73 to 25.41%, indicating the negative correlation between them (Figure 5B).

## Hormones in Serum and Testis

With the development of the testes, the content of T3 gradually increased. It rose significantly at the stage of V(2500 g) and

peaked at the stage of VI(2500 g), then it descended at the stage of VI+(2500 g) after the breeding activity (Figure 6Aa). The content of 5-HT significantly increased when the gonad matured at the stage of IV(2200 g) after a brief decline around the stage of II(400 g) and II(800 g) (Figure 6Ab). The content of E2 showed an “M”-like curve, with a high concentration at the stage of II(80 g) and a top level at the stage of V(2500 g). Thereafter, it decreased to the initial level at the stage of V+(2500 g). The content of E3 had a similar trend with E2, but the changes were less obvious

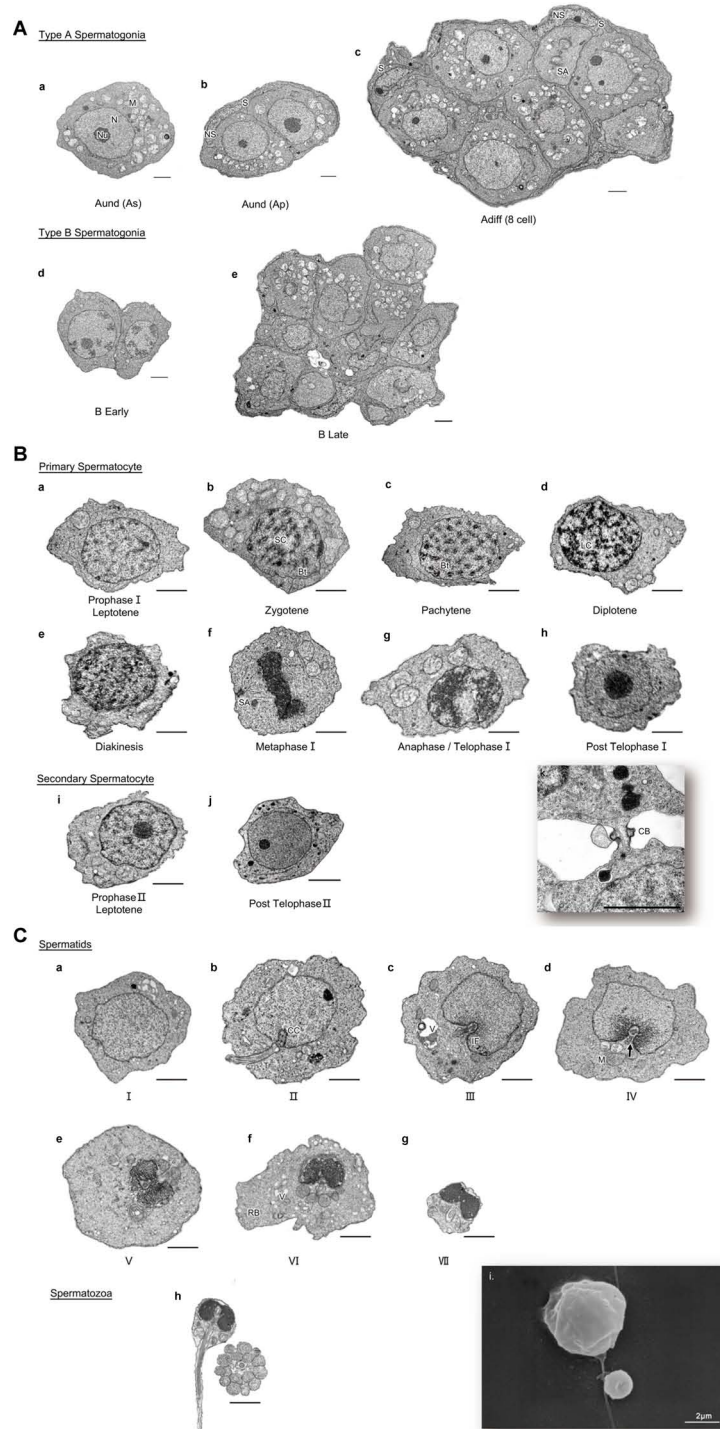


**FIGURE 3 | (A)** Different developmental stages of spermatogonia. **(a-c)** type A spermatogonia; **(a)** type A undifferentiated spermatogonia (single) [Aund (As)]; **(b)** type A undifferentiated spermatogonia (paired) [Aund (Ap)]; **(c)** type A differentiated spermatogonia [Adiff (8cell)]; **(d,e)** type B spermatogonia; **(d)** B Early; **(e)** B Late. N, nucleus; Nu, nucleolus; M, mitochondria; S, Sertoli cell; NS, nucleolus of Sertoli cell; SA, spindle apparatus. TEM. Scale bar 2  $\mu\text{m}$ .  $n = 6$ . **(B)** Different developmental stages of spermatocyte. **(a-h)** primary spermatocyte; **(a)** Prophase I Leptotene; **(b)** Prophase I Zygotene; **(c)** Prophase I Pachytene; **(d)** Prophase I Diplotene; **(e)** Prophase I Diakinesis; **(f)** Metaphase I; **(g)** Anaphase/Telophase I; **(h)** Post Telophase I; **(i,j)** secondary spermatocyte; **(i)** Prophase I Leptotene; **(j)** Post Telophase II; **(k)** cytoplasmic bridge between two spermatocytes. SC, synaptonemal complex; Bt, bivalent; LC, lampbrush chromosome; SA, spindle apparatus; CB, cytoplasmic bridge. TEM. Scale bar 2  $\mu\text{m}$ .  $n = 6$ . **(C)** Process of spermiogenesis showed different stages of spermatids and spermatozoa. **(a-g)** Spermatid I – VII; **(h)** Spermatozoa; **(i)** SEM of Spermatid III and Spermatozoa. CC, centrosome complex; T, tail; IF, implantation fossa; V, vesicle; M, mitochondria; RB, residual body; arrow: central space of sleeve. TEM, SEM. Scale bar 2  $\mu\text{m}$ .  $n = 6$ .

**TABLE 2** | Morphological changes, cell diameter, and nuclear diameter of germ cells at different stages.

		Nuclear diameter ( $\mu\text{m}$ )	Cell diameter ( $\mu\text{m}$ )	Major morphological changes	Figures number
Spermatogonia	Aund (As)	$7.00 \pm 0.51$	$12.34 \pm 0.74$	– The largest germ cell, with very low electron density and regular outlines. A large nucleus with clear nuclear membrane boundaries, and 1 – 2 obvious large nucleoli. The cytoplasm was insufficiently differentiated and had an irregular shape. A large number of mitochondria were around the nucleus. Each Aund (As) was wrapped by 1 or 2 Sertoli cells, independent from the other germ cells.	<b>Figure 3Aa</b>
	Aund (Ap)	$6.09 \pm 0.63$	$10.12 \pm 1.33$	– Very similar to Aund (As), but smaller.	<b>Figure 3Ab</b>
	Adiff (8cell)	$5.74 \pm 0.38$	$9.36 \pm 0.89$	– A spermatocyst usually contained 6–8 Adiff (8 cell). Smaller in size, with several obvious nucleoli. The nuclear membrane boundary was clear. The cytoplasm contained a large number of mitochondria.	<b>Figure 3Ac</b>
	B Early	$5.16 \pm 0.76$	$8.80 \pm 1.24$	– The process of Adiff (8 cell) transformed to B Early was irreversible. A spermatocyst usually contained 16 or more B Early. Oval nucleus, in which heterochromatin and 1 – 2 smaller nucleolus could be observed.	<b>Figure 3Ad</b>
	B Late	$4.82 \pm 0.34$	$8.09 \pm 0.93$	– The number of B Late inside a spermatocyst was significantly increased.	<b>Figure 3Ae</b>
Primary spermatocyte	Prophase I Leptotene	$4.60 \pm 0.48$	$6.75 \pm 0.53$	– The chromosomes were shaped in thin lines with rosary chromatin. The chromosomes were replicated during this period, but the two chromatids could not be distinguished under the electron microscope, only showed a preliminary deepening of chromatin staining in the nucleus.	<b>Figure 3Ba</b>
	Prophase I Zygotene	$4.90 \pm 0.45$	$7.70 \pm 0.91$	– There was a typical developmental event called synapsis, during which the paired homologous chromosomes formed a synaptonemal complex (SC). Under the electron microscope, the synaptonemal complex was clearly observed, with two deeper chromosomes bonding together, and arranging in parallel, which was called bivalent body.	<b>Figure 3Bb</b>
	Prophase I Pachytene	$4.96 \pm 0.51$	$7.09 \pm 0.61$	– The bivalent bodies became shorter, tightly bound, darkly colored, and evenly distributed in the nucleus. The non-sister chromatids of homologous chromosomes started crossing over.	<b>Figure 3Bc</b>
	Prophase I Diplotene	$4.19 \pm 0.59$	$6.28 \pm 1.04$	– The synaptonemal complex disappeared. The bivalent bodies untwisted and the homologous chromosomes began to uncoil each other for separation. The chromosomes further shortened to form the lampbrush chromosomes, which were deeply colored and visualized like lampbrushes under TEM. Compared to the three stages in former, this period was more difficult to observe.	<b>Figure 3Bd</b>
	Prophase I Diakinesis	$3.95 \pm 0.44$	$5.53 \pm 0.43$	– The chromosomes were even shorter, spread evenly in the nucleus, and tended to move toward the periphery of the nucleus. This phase was also difficult to observe.	<b>Figure 3Be</b>

(Continued)

TABLE 2 | Continued

		Nuclear diameter ( $\mu\text{m}$ )	Cell diameter ( $\mu\text{m}$ )	Major morphological changes	Figures number
	Metaphase I		$5.09 \pm 0.39$	– The nucleolus disappeared, the nuclear membrane disintegrated, and the chromosomes lined up on the equatorial plane. Due to the deep coloration and dense spatial arrangement, the boundaries between chromosomes could not be clearly observed. A deeply colored rectangle-like structure formed on the equatorial plane. The chromosome was pulled by the spindle apparatus and centrosome.	<b>Figure 3Bf</b>
	Anaphase/Telophase I	$2.99 \pm 0.03$	$4.80 \pm 0.16$	– The two homologous chromosomes of the divalent bodies separated and moved toward the poles of the cell. Once chromosomes reached the poles, they unwound into filaments. Then the nuclear membrane rebuilt, and the cytokinesis continued. This stage was also difficult to observe under TEM.	<b>Figure 3Bg</b>
	Post Telophase I	$3.32 \pm 0.13$	$4.43 \pm 0.23$	– The nuclear membrane rebuilt with a large nucleolus. The cytoplasm was few just after the cell division.	<b>Figure 3Bh</b>
Secondary Spermatocyte	Prophase II Leptotene	$2.88 \pm 0.18$	$4.37 \pm 0.16$	– The cell was smaller than Prophase I Leptotene, with a filamentous and darkened chromatin.	<b>Figure 3Bi</b>
	Post Telophase II	$2.71 \pm 0.12$	$4.25 \pm 0.21$	– MeiosisII was complete, the nuclear membrane rebuilt, and the nucleolus reappeared.	<b>Figure 3Bj</b>
Spermatid	SpermatidI	$3.84 \pm 0.32$	$5.48 \pm 0.75$	– There were a few heterochromatins appeared in the nucleus, the coloration around the double-layered nuclear membrane gradually deepened. The nascent flagellar did not form yet.	<b>Figure 3Ca</b>
	SpermatidII	$3.65 \pm 0.55$	$5.81 \pm 0.46$	– The spermatids were irregular in shape and their bilayer membrane structure was clear, with a large number of mitochondria and vesicles in the cytoplasm. The early centrosome complex formed in the nucleus near the cell membrane, consisting of proximal centriole, intercentriolar body, and distal centriole. The proximal centriole was close to the nuclear membrane, which formed a certain angle with the distal centriole. The flagellum (in the form of "9 + 2") extended at the base of the proximal centriole to form the original sperm tail. The base of the original tail was flush with the edge of the nucleus, and without being sunken into the nucleus.	<b>Figure 3Cb</b>
	SpermatidIII	$3.45 \pm 0.22$	$6.11 \pm 0.33$	– The spermatids were irregular in shape, with increasing size. The centrosome complex became more mature. The base of the sperm tail recessed into the nucleus (about 1/3 of the nucleus) to form implantation fossa. The chromatin started to concentrate toward the side of sperm tail. The nucleus near the implantation fossa became granular with deepened coloration	<b>Figure 3Cc</b>

(Continued)

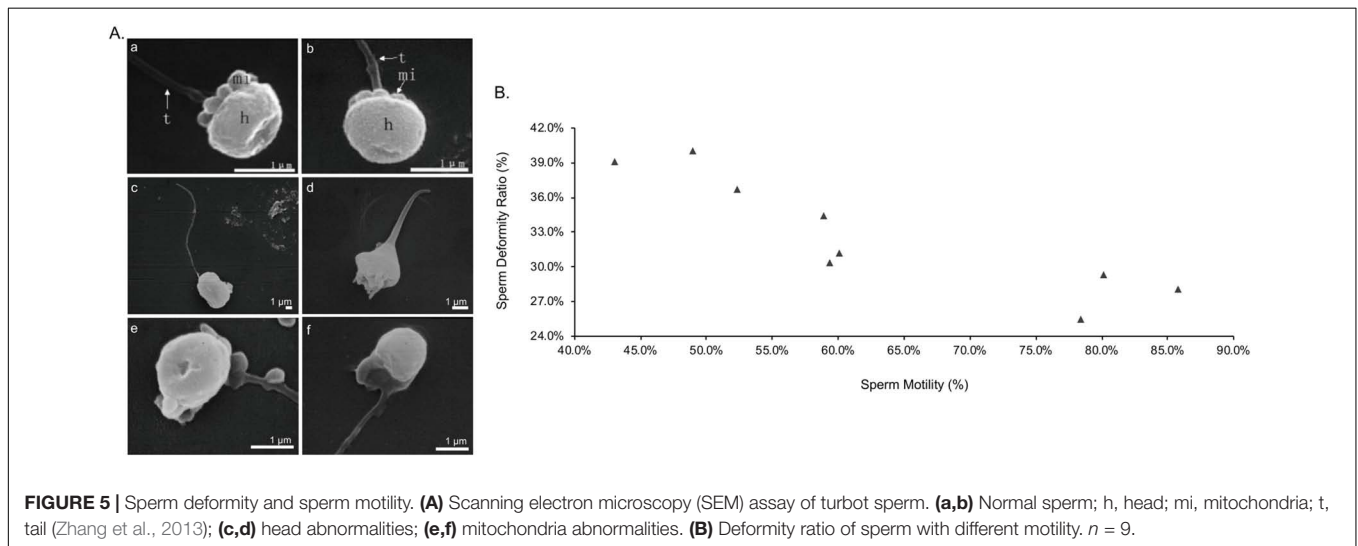
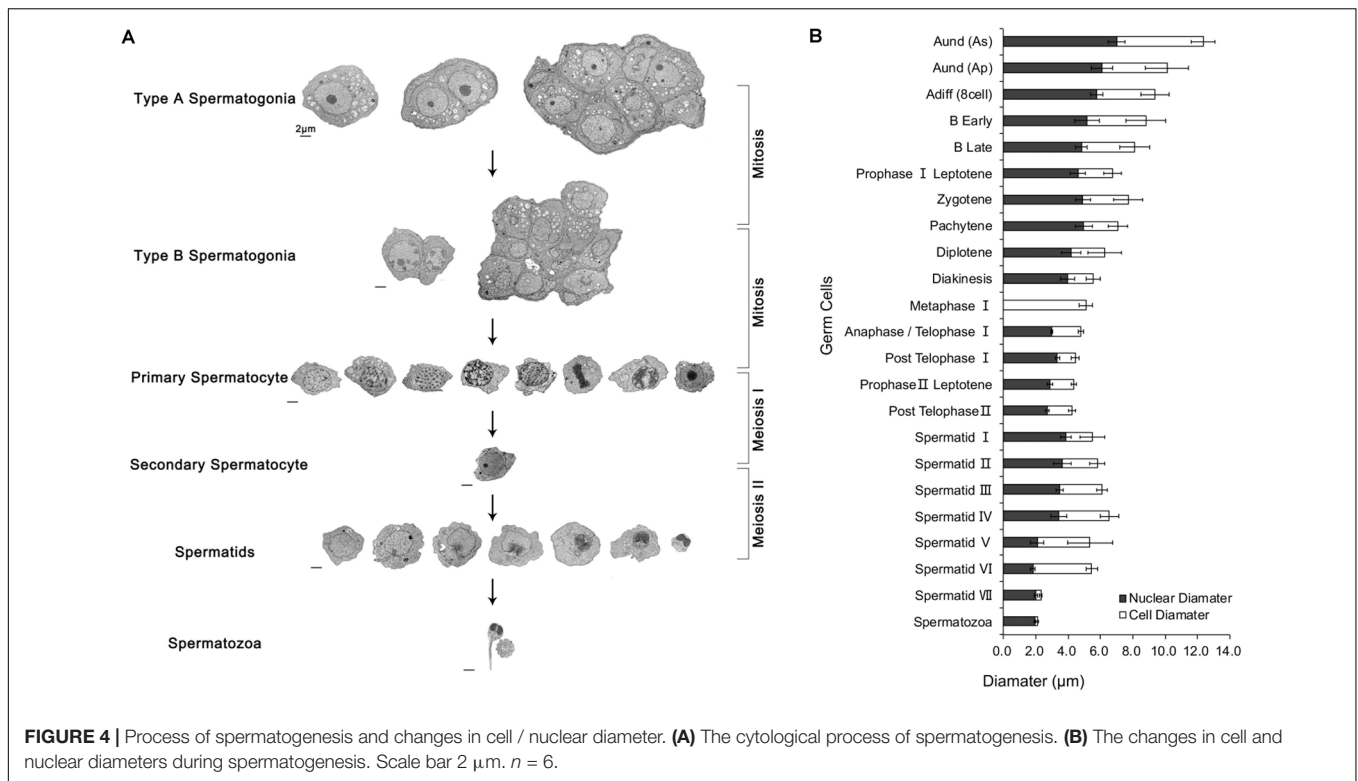
TABLE 2 | Continued

		Nuclear diameter ( $\mu\text{m}$ )	Cell diameter ( $\mu\text{m}$ )	Major morphological changes	Figures number
	SpermatidIV	$3.41 \pm 0.49$	$6.53 \pm 0.57$	<ul style="list-style-type: none"> <li>– The centrosome complex rotated. The angle between the proximal centriole and the distal centriole disappeared.</li> <li>– The implantation fossa recessed more deeply into the nucleus (about 1/2 of the nucleus).</li> <li>– The flagellum and the cell membrane at the edge of the nucleus formed a narrow cavity, which is called the central space of sleeve.</li> <li>– Approximately 8 – 9 dense linear substances neatly located in the cytoplasm around the front part of the flagellum. The cross section of this structure appeared as 8 – 9 dense particles roughly arranged in a circle, which is called as flagellar satellite complex.</li> <li>– The nucleus concentrated toward the tail side, large mitochondria appeared in the cytoplasm and gradually moved toward the base of the tail.</li> </ul>	<b>Figure 3Cd</b>
	SpermatidV	$2.08 \pm 0.41$	$5.35 \pm 1.40$	<ul style="list-style-type: none"> <li>– The electron density of the chromatin in the nucleus significantly increased.</li> <li>– The chromatin was sharply condensed and transformed into coarse particles, and the nucleus volume significantly reduced, leading to the preliminary formation of the sperm nucleus.</li> <li>– Large mitochondria began to assemble at the base of the tail.</li> <li>– Vesicles continued to increase and vacuolated in other areas of the cytoplasm (residual body).</li> </ul>	<b>Figure 3Ce</b>
	SpermatidVI	$1.81 \pm 0.15$	$5.46 \pm 0.36$	<ul style="list-style-type: none"> <li>– The electron density of the chromatin continued to increase, and 2 - 3 nuclear membrane layers formed.</li> <li>– Large mitochondria kept assembling around the base of the tail.</li> <li>– The cavitation and deformation of the residual body were intensified, and the residual bodies started move toward the tail and gradually separated from the main spermatid.</li> </ul>	<b>Figure 3Cf</b>
	SpermatidVII	$1.99 \pm 0.11$	$2.30 \pm 0.09$	<ul style="list-style-type: none"> <li>– The nucleus was further concentrated, but partial vacuoles could still be observed.</li> <li>– Most of the residual bodies fell off, leaving the rest parts gathered under the nucleus.</li> <li>– The volume of mitochondrial increased to the maximum.</li> </ul>	<b>Figure 3Cg</b>
Spermatozoa	Spermatozoa	$1.94 \pm 0.08$	$2.08 \pm 0.06$	<ul style="list-style-type: none"> <li>– The nucleus concentrated into a homogeneous substance with a high electron density, in which scattered vacuoles could be observed.</li> <li>– The residual bodies had completely fallen off, the mitochondria were fully assembled.</li> <li>– A spermatozoon contained at least 16 spherical mitochondria.</li> </ul>	<b>Figure 3Ci</b>

(**Figure 6Ac**). Compared to the 11-KT, the content of T increased at the stages of IV(2200 g) and V(2500 g) before falling back to the initial level (**Figure 6Ad**). The concentration of  $17\alpha,20\beta$ -DHP was high during the stage of II(15 g) and the mature stages from V(2500 g) to VI(2500 g). Moreover, the content of P4 exhibited a similar trend as that of  $17\alpha,20\beta$ -DHP, with a high level at the stage of II(15 g), II(400 g), and V(2500 g) (**Figure 6Ae**). During the mature stages from IV(2200 g) to V(2500 g), the serum concentrations of T3, 5-HT, T,  $17\alpha,20\beta$ -DHP and E2 all increased, and the changes

of T content was the most noticeable, with an increase of ~57-fold.

In order to investigate if the changes of hormone levels in the testis were similar to those in the serum, we examined the testis concentrations of T/11-KT and  $17\alpha,20\beta$ -DHP/P4 at different stages (**Figures 6Bf,g**). The dominance of T content in the serum seemed to be compromised in the testis, which was replaced by an overall high level of 11-KT. The highest concentration of T occurred at the early stage of II(400 g). While 11-KT maintained a relatively higher level, with a high

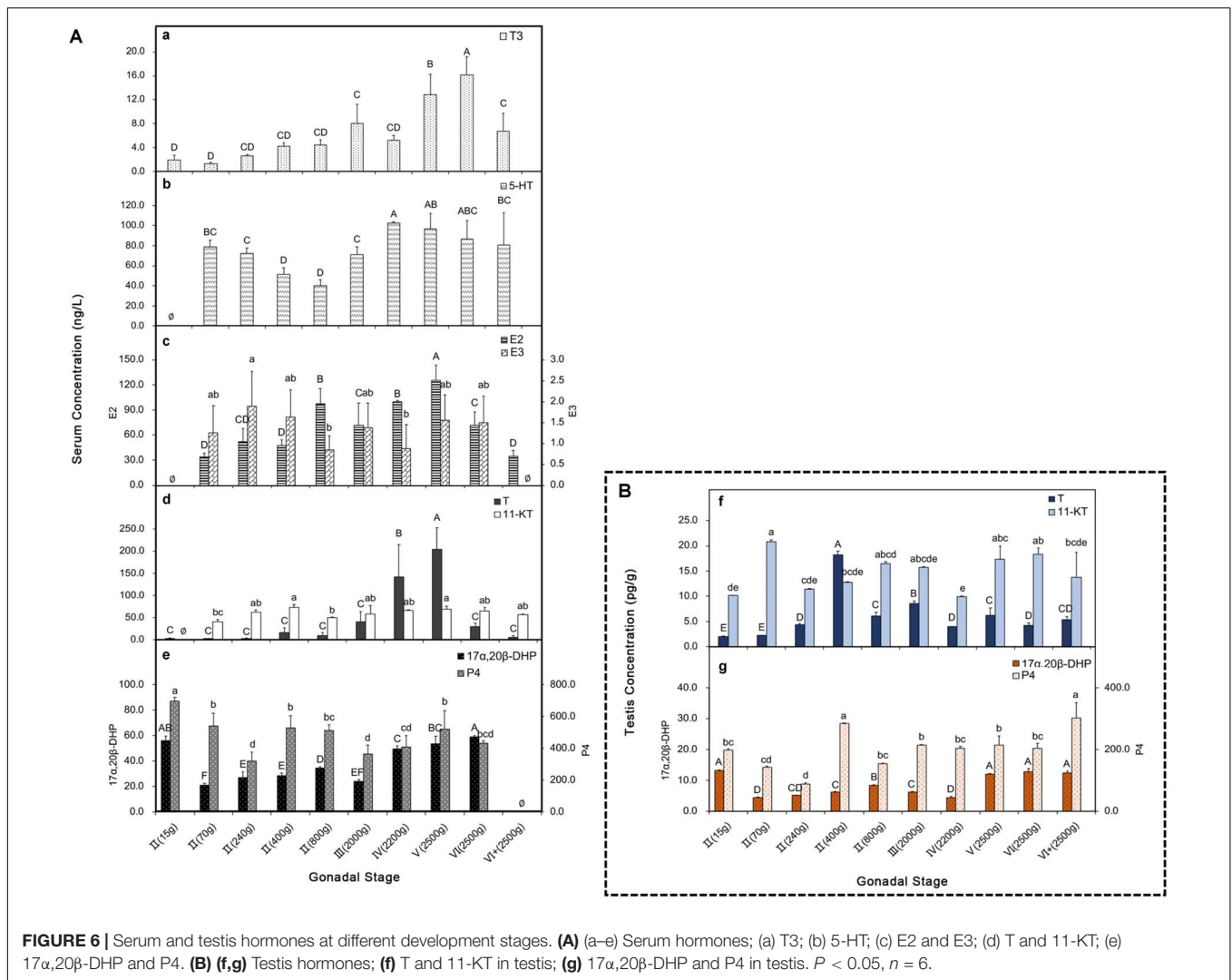


content at the stages of II(70 g) and VI(2500 g) (**Figure 6Bf**). The concentration of  $17\alpha,20\beta$ -DHP in the testis was similar to that in the serum, which was high at both the early stage of II(15 g) and the mature stages from V(2500 g) to VI+(2500 g). The P4 content exhibited a roughly similar trend as that in the serum, with a particularly high concentration at the stage of II(400 g) (**Figure 6Bg**).

## Expression and Location of AR mRNA

In order to explore more details about the androgens, we cloned the cDNA fragment of androgen receptor (AR) and examined

its intra-gonadal expression and localization (**Figure 7**). The AR gene highly expressed at the early stages of II(15 g) and II(70 g), while afterward, it gradually declined until the stage of IV(2200 g). Then, it rebounded from the stage of IV(2200 g) to V(2500 g) (**Figure 7A**). To facilitate the localization of AR, we used *Sox9* as a marker for Sertoli cells (somatic cells of spermatogenic epithelium). The results of FISH showed that, the mRNA of AR mainly expressed in but not limited to the edge of the spermatocysts, where Sertoli cells also concentrated. The signal was weaker in matured spermatids and spermatozoa (**Figure 7B**).



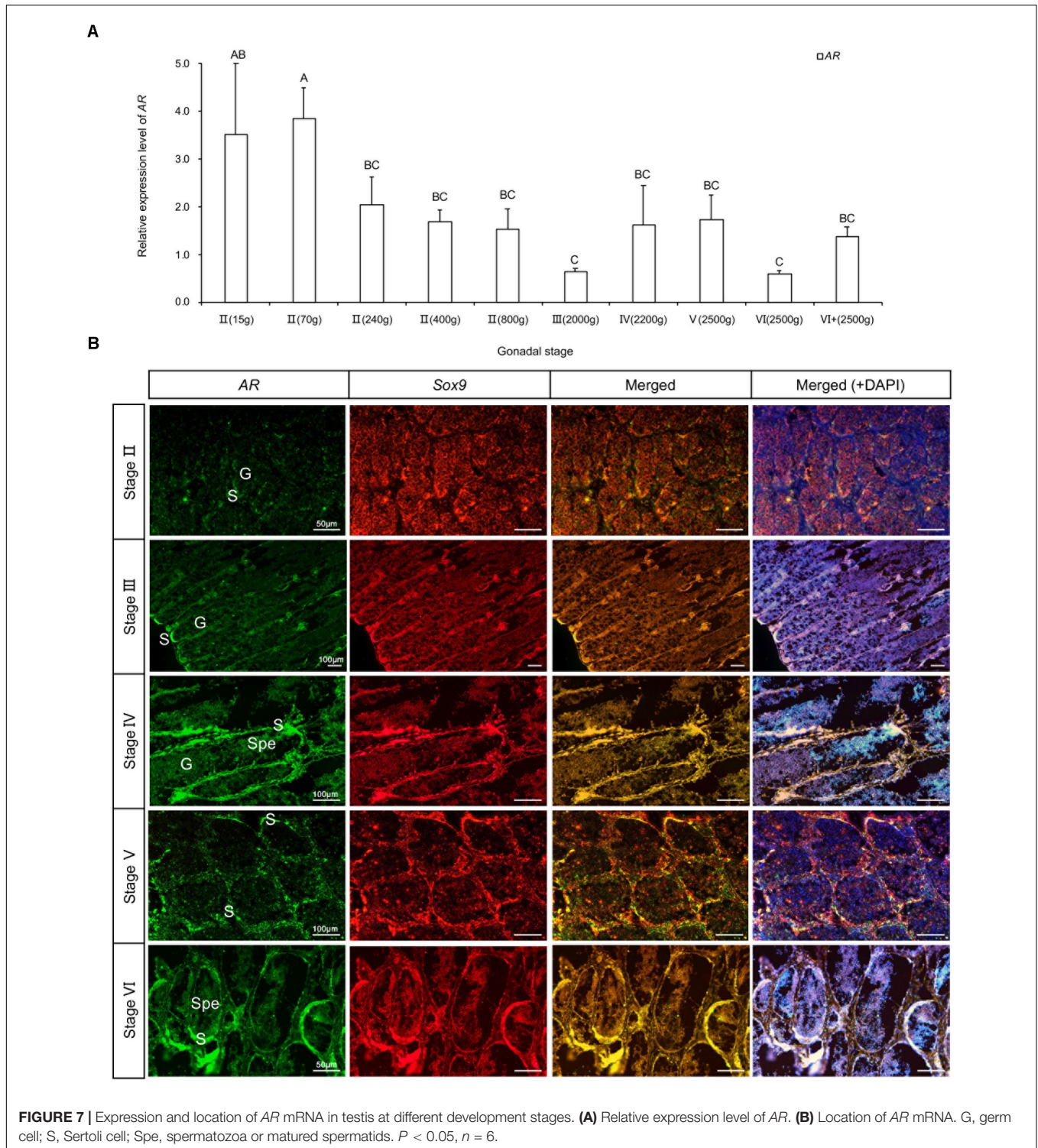
## DISCUSSION

In the present study, the development period was throughout the initiation and the entire adult breeding season, including samples about 2.5 months after the breeding period [stage VI+(2900 g)].

There is a widespread consensus that only Aund (As) has the properties of stem cells, which is Spermatogonial Stem Cells (SSCs) in the true sense. SSCs are self-renewal to maintain a constant number in the testis. Triggered by external signals, they can also proliferate and differentiate into the next stage of germ cells and eventually develop to mature sperm. In this study, we found that in turbot, each Aund (As) was wrapped by 1 or 2 Sertoli cells. These somatic cells isolated Aund (As) from the other non-SSCs, forming a stable internal environment. In mammals, Aund (Ap) is transformed from Aund (As) by mitosis, and the cytoplasmic bridge was found to exist in different stages of germ cells, such as undifferentiated spermatogonia (Schulz et al., 2010), spermatocytes (Greenbaum et al., 2011), spermatids (Ventelä et al., 2003), etc. In the

present study, we observed the cytoplasmic bridge between spermatocytes (Figure 3Bk), which agreed with the findings in mouse (pachytene and secondary spermatocytes) (Greenbaum et al., 2011). Moreover, we also found that both type A and type B spermatogonia in the anaphase of mitosis and showed their respective dynamics of transformation into their next developmental stage [Adiff (8 cell) to B Early; B Late to primary spermatocytes].

Although spermatocytes in different phases of meiosis can be identified based on the cell characteristics, such as cell and nuclear size and chromosome condensation, few systematic studies focused on the meiosis phases of spermatogenesis in bony fishes (Leal et al., 2009). Here we first observed the relatively complete phases of primary spermatocytes, and we were fortunate to discover multiple typical development stages in male turbot, although several periods were rare due to their short duration. Based on these, we speculated that the potential relationship between different development phases for turbot was similar to that in mammals (Bruce et al., 2002), yet still need more studies for validation.



Spermiogenesis is a highly organized developmental process for structural rebuilding and functional maturation of spermatids, which was easily ignored by the previous studies of fish spermatogenesis. According to the available literature, the method of dividing the developmental stages of spermatids is not consistent, and the appearance time of the sperm tail is

unclear. For stone flounder, spermatids were divided into two stages, the early and late stages, with the flagellum formed in the late stage (Kang et al., 2016). For zebrafish, spermatids were divided into three stages, including initial (E1), intermediate (E2), and final (mature) (E3) steps (Leal et al., 2009). The division based on the increasing nuclear compaction and

space between the spermatids, which reflected the loss of cytoplasmic bridges and the formation of flagellum. The process of spermatogenesis in silver pomfret (Chung et al., 2010) and mudskipper (*Boleophthalmus pectinirostris*) (Chung, 2008) was also divided into three steps, with the flagellum formed at the final stage. For pacu (*Piaractus mesopotamicus*), one early spermatid (sd) and two stages of more mature spermatids (zp1 and zp2) were described according to their nuclei condensation, with the flagellum formed in the late spermatids (da Cruz-Landim et al., 2003). In Senegalese sole (*Solea senegalensis*), used molecular markers to separate stages during spermatozoa differentiation, the spermatogenesis was divided into four steps: round spermatids, differentiating spermatids, condensed spermatids and spermatozoa. Immunostaining for  $\alpha$ -tubulin showed that the protein was restricted to half of the cytoplasm in differentiating spermatids, and to the nascent flagellar region in the condensing stage (Chauvigné et al., 2014b). Multiple studies on fishes have assumed that sperm tail appears around the final stage of spermiogenesis. However, here we found that in turbot, the sperm tail formed in early spermiogenesis (Spermatid II), and it might play an important role in the subsequent removal of residual bodies and mitochondrial localization, which was in line with the research outcomes based on mammals (Lehti and Sironen, 2016, 2017). In mouse, disrupted the assembly of microtubules can cause the failure of the proper sperm tail assembly, the acrosomes formation, and the inappropriate removal of the residual bodies, resulting in the aberrant formation of sperm cells and subsequent sperm cell apoptosis (Tang et al., 2016; Lehti and Sironen, 2017). When we look back on earlier research, similar results were also reported in Nile tilapia, the spermatid differentiation process of which was divided into six stages, with straight flagellum began to rise from the distal centriole and nearly perpendicularly extends beyond the plasma membrane during the first stage (Lou and Takahashi, 1989). And it corresponded to the stage of Spermatid II in the present study. A recent study on Adriatic sturgeon (*Acipenser naccarii*) also showed that the flagellum occurred in early spermatids, although spermiogenesis was not clearly divided (Grandi et al., 2018).

In the present study, the head diameter and the number of mitochondria of the spermatozoa were revised according to the previous study of our team (Zhang et al., 2013). With the development of the germ cells, the cell and nucleus volume gradually declined except for the stages around primary spermatocyte Prophase I Zygotene and early spermiogenesis, possibly due to the vigorous intracellular physiological activities and anabolic metabolism.

It is well accepted that better semen tends to have fewer abnormal sperm (Miciński et al., 2011). The result of sperm deformity hindering motility in turbot prompted us to further systematically examine the detailed process of spermatogenesis, including the hormones and the gene expressions.

In the early 21st century, T3 was revealed to regulate the growth and maturation of the testis of mammals, including influencing the proliferation and differentiation of Sertoli cells and Leydig cells (Holsberger et al., 2005; Mendis-Handagama and Siril Ariyaratne, 2005). T3 also participates in the steroidogenesis

(e.g., the synthesis of T and E2) (Maran et al., 2000; Fallah-Rad et al., 2001; Hernandez, 2018). For a long time, T3 is mainly recognized to function during early testis development at prepubertal age. Later, a study based on rats found that the expression of type 2 deiodinases (an enzyme that plays a major role in the intracellular conversion of T4 to T3s) was high in elongated spermatids, rather than in other germ cells or Sertoli cells. This suggested that T3 is also critical for the maturation process of the testis, specifically during spermiogenesis (Wagner et al., 2008). Our results suggested that in fish, T3 also played an important role in sperm maturity.

An increasing evidence suggests that estrogens involve in both the spermatogenesis and the regulation of testicular functions (Schulz et al., 2010; Björn et al., 2013). Estrogen receptors have been identified in testis (Dumasia et al., 2016; Kumar et al., 2018), and they generally respond to the secretion of E2 differ between developmental stages of the gonads and different organs (Hyeon et al., 2019). However, estrogens in the testis are produced by Leydig cells, Sertoli cells, and germ cells through the aromatization of testosterone, and they are very active during puberty initiation (Amer et al., 2001; Takeshi and Chiemi, 2003) and spermatogenesis (Munakata and Kobayashi, 2010; Björn et al., 2013; Kumar et al., 2018). A recent study of gilthead seabream (*Sparus aurata*) suggesting that the potential interplay of E2 and progestin pathways for the maintenance of spermatogonial renewal (Chauvigné et al., 2017). In the present study, compared to E3, the content of E2 was more strongly correlated with the early stage of spermatogenesis and spermiogenesis, which was in accordance with the previous studies on gilthead seabream (Chauvigné et al., 2017) and pikeperch (*Sander lucioperca*) (Björn et al., 2013).

In mammals, 5-HT was found to regulate testosterone synthesis and sperm development both *in vivo* and *in vitro* (Csaba et al., 1998; Frungieri et al., 2002; Gerendai et al., 2007). The malfunction of 5-HT would disrupt the hormonal communication between testis and hypophysis (Díaz-Ramos et al., 2018), reduce semen quality, and even compromise the integrity of sperm DNA (Safarinejad, 2008; Martin et al., 2019). Similarly, in fishes, the increased 5-HT concentration can stimulate the release of gonadotropin-releasing hormones (GnRHs) (McDonald, 2017), gonadotropic hormones (GTHs) (Kreke and Dietrich, 2008), and androgens (Bertil, 1994; Munakata and Kobayashi, 2010), which directly regulates spermatogenesis. In the present study, we found that the 5-HT had high levels at the stages of II(70 g) and IV(2200 g). The former might relate to the rapid development following testis initiation, while the latter might relate to the maturation of the sperm cells (spermiogenesis) and the active breeding activities. In addition, estrogens were also detected to affect the levels of 5-HT in serum and its receptors in the brain (Luine and Rhodes, 1983; Meston and Gorzalka, 1992; Fink et al., 1999), which agreed with our findings in this study.

The androgens T and 11-KT are recognized to control the spermatogenic cycle in fishes (Weltzien et al., 2004; Schulz et al., 2008, 2010; Kloas et al., 2009). The hormone T is important for the differentiation at the early stages through promoting the proliferation of spermatogonia for spermiogenesis, whereas 11-KT mainly regulates the initiation

of spermatogonial proliferation toward meiosis (Weltzien et al., 2004; Munakata and Kobayashi, 2010; Björn et al., 2013), and partly regulates the final maturation of gametes (Schulz et al., 2010; Taranger et al., 2010). In flatfish Senegalese sole and brill (*Scophthalmus rhombus*), 11-KT in plasma increased just before or during the spermiation time (Hachero-Cruzado et al., 2013; Chauvigné et al., 2016). In the present study, the contents of T and 11-KT in serum both increased, while only T prominently changed during the mature stages [IV(2200 g) – V(2500 g)], which was highly consistent with the situation at the stages of spermiogenesis, indicating that T might be crucial during the mature period of turbot. Similar profiles were also found in halibut (*Hippoglossus hippoglossus*), kutum roach (*Rutilus frisiiikutum*), gilthead seabream and walleye (*Stizostedion Vitreum*) (Malison et al., 1994; Weltzien et al., 2002; Bani et al., 2015; Boj et al., 2015). For halibut, both T and 11-KT contents increased at the stages of haploid germ cells, including spermatozoa (Stage III and IV) (Weltzien et al., 2002), which corresponded to the stages of IV(2200 g) and V(2500 g) in our study. These results make us curious about the situation in the testis. We found the peak of T content in the testis occurred during the early stage, while the dominance during the mature stages weakened. On the contrary, the trend of 11-KT content in the testis was more or less similar to that in the serum, which was relatively high in both the early and mature stages. It seems that the changing patterns of androgens during spermatogenesis are varied among species.

In male fish, progestins were found to induce spermiation (Ueda et al., 1985), and stimulate the production and motility of sperm (Miura et al., 1992; Tubbs and Thomas, 2008). The role of DHP during spermiation is known for a long time, enhancing sperm motility (by alteration of the pH and fluidity of the seminal fluid) and acting as a pheromone in male cyprinids (Scott et al., 2010). Besides, the DHP was also found to promote the proliferation and differentiation of early spermatogonia (Chen et al., 2013) and induce the meiosis of germ cells (Miura et al., 2006). In our study, P4 and DHP, especially the latter one, had relatively higher concentrations during the early stages and spermiogenesis, indicating the similar function of these hormones in male turbot.

Although the sperm excretion and ovulation cannot be naturally achieved under factory culturing conditions, reproductive activities of male turbot in chasing female turbot can still be observed at breeding season, and the yield and vitality of sperm maintain at certain levels, which has a close relationship with the sex steroid levels. The serum concentrations of T3, 5-HT, T, 17 $\alpha$ ,20 $\beta$ -DHP, and E2 showed significant correlations with spermiogenesis from stage IV(2200 g) to stage V(2500 g). In fact, a large number of studies also show the regulatory relationship among these hormones. Overall, our findings are corroborative to each other, which delineated the characteristics of hormone changes during the spermatogenesis of turbot.

The differences in the contents of T and 11-KT between the serum and testis facilitated us to examine the functional roles of androgens in the spermatogenesis of turbot. Therefore, we cloned the potential ligand AR to examine its expression and distribution (Figure 7). We found that the expression of AR at

the early stages was roughly consistent with the changes of 11-KT in the testis and was ahead to the changes of T. Besides, the expression of AR during spermiogenesis was similar to the changes of T in the serum. In subsequent research we found that the fluorescence signal of AR mainly located in but not limited to the Sertoli cells-concentrated area. In mammals, AR located in various types of cells, including Sertoli cells, Leydig cells, peritubular myoid cells and germ cells (Walters et al., 2010). The FISH analysis of zebrafish testis revealed that AR mRNA expressed in the subpopulation of Sertoli cells around early spermatogonia (de Waal et al., 2008). For bonnethead shark (*Sphyrna tiburo*), AR mRNA expressed in multiple cell types of cells in the male bonnethead testis (premeiotic germ cells, Leydig-like interstitial cells, Sertoli cells, peritubular myoid cells, and mature spermatozoa) and gonadal ducts (stromal cells, luminal epithelial cells, and mature spermatozoa). For Senegalese sole, the nuclear ARs AR $\alpha$  expressed in germ cells (spermatogonia, spermatocytes, and spermatids), whereas the AR $\beta$  expressed in Sertoli cells (Chauvigné et al., 2014a). Moreover, in the nearly mature spermatocysts containing elongating spermatids, strong AR immunoreactivity was detected in Sertoli cells (Tyminski et al., 2015). Our results of AR were quite consistent with the previous studies, suggesting the similar function of AR in regulating spermatogenic epithelium and the potential crosstalk between Sertoli cells and germ cells in turbot. Whereas, more detailed regulatory mechanism still needs future investigations.

Based on our results, the facts that affect the sperm quality of cultured turbot could be varied. One is the sperm deformity we found in the present study. There are many causes of sperm deformity. It might due to abnormal hormone regulation, especially the steroid hormones such as T and 11-KT, which need to be further verified by more experiments. Moreover, our results showed that even 2.5 months after the breeding season, spermatozoa and spermatids can still be found in the testis, suggesting that the aging of germ cells may also be a problem that cannot be ignored. It matters especially for the fish species that require artificial insemination. For the farmworkers in the turbot aquaculture industry, regulating the synchronous development of the gonads as much as possible may be the best way to avoid sperm deformities and sperm quality degradation. Finally, it is necessary to pay attention to the changes of hormone levels of the broodstock, and provide necessary manual intervention, especially during the matured stages from stage IV(2200 g) to V(2500 g).

## CONCLUSION

In the present study, we examined a great number of different developmental stages to fully display the spermatogenesis developmental process of turbot. Generally, the aqua-cultured turbot undergoes a normal spermatogenesis process. The detailed cytology and main hormone changes throughout the reproductive cycle are first revealed. The differential expressions of T and 11-KT at both hormone and mRNA levels suggest their potential diverse functions at different development stages.

## DATA AVAILABILITY STATEMENT

The raw data supporting the conclusions of this article will be made available by the authors, without undue reservation.

## ETHICS STATEMENT

The animal study was reviewed and approved by Experimental Animal Ethics Committee, Institute of Oceanology, Chinese Academy of Sciences, China.

## AUTHOR CONTRIBUTIONS

YL: experiment design, experiment implementation, and manuscript writing. QL: experiment design and manuscript revision. SX and YW: experimental broodstock culture and sampling. CF and CZ: assistance with sampling and experiment implementation. ZS: provide aquaculture facilities and broodstock. JL: research management, experiment design, assistance with implementation, interpretation, and manuscript submission. All authors contributed to the article and approved the submitted version.

## FUNDING

This research was supported by the National Natural Science Foundation of China (Nos. 31702321, 31572602, and 31802319), Zhejiang Provincial Natural Science Foundation of China (No. LY20C190008), Shandong Province Major Science

and Technology Innovation Project (No. 2018SDKJ0302-4), Shandong Province Key R&D Projects (No. 2019GHY112013), Natural Science Foundation of Shandong Province (No. ZR2018BC053), National Key Research and Development Program (No. 2018YFD0901204), Key Special Project for Introduced Talents Team of Southern Marine Science and Engineering Guangdong Laboratory (Guangzhou) (No. GML2019ZD0402), Major Agricultural Application Technology Innovation Project of Shandong Province (No. SD2019YY011), Qingdao National Laboratory for Marine Science and Technology (No. 2018SDKJ0502-2), China Agriculture Research System (No. CARS-47), Major Science and Technology for Scientific and Technological Innovation Projects (Shandong) (No. 2019JZZY020710), and STS Project (Nos. KFZD-SW-106, ZSSD-019, 2017T3017, and 2019T3022).

## ACKNOWLEDGMENTS

We thank all the members of the laboratory for their technical advice and helpful discussions.

## SUPPLEMENTARY MATERIAL

The Supplementary Material for this article can be found online at: <https://www.frontiersin.org/articles/10.3389/fmars.2020.592880/full#supplementary-material>

**Supplementary Figure 1** | Different developmental stages of turbot testis. H&E. Scale bar 500  $\mu\text{m}$  (4x), 10  $\mu\text{m}$  (40x).  $n = 6$ .

## REFERENCES

- Amer, M. A., Miura, T., Miura, C., and Yamauchi, K. (2001). Involvement of sex steroid hormones in the early stages of spermatogenesis in Japanese huchen (*Hucho perryi*). *Biol. Reprod.* 65, 1057–1066. doi: 10.1095/biolreprod65.4.1057
- Bani, A., Haghi Vayghan, A., and NaserAlavi, M. (2015). The effects of salinity on reproductive performance and plasma levels of sex steroids in *Caspian kutum Rutilus frisii kutum*. *Aquac. Res.* 47, 3119–3126. doi: 10.1111/are.12762
- Benini, E., Politis, S. N., Kottmann, J. S., Butts, I. A. E., Sørensen, S. R., and Tomkiewicz, J. (2018). Effect of parental origin on early life history traits of European eel. *Reprod. Domest. Anim.* 53, 1149–1158. doi: 10.1111/rda.13219
- Bertil, B. (1994). Androgens in teleost fishes. *Comp. Biochem. Physiol. C Toxicol. Pharmacol.* 109, 219–245. doi: 10.1016/0742-8413(94)00063-G
- Björn, H., Sven, W., Bernhard, R., Werner, K., and Carsten, S. (2013). Temperature control of pikeperch (*Sander lucioperca*) maturation in recirculating aquaculture systems - induction of puberty and course of gametogenesis. *Aquaculture* 400–401, 36–45. doi: 10.1016/j.aquaculture.2013.02.026
- Boj, M., Chauvigné, F., Zapater, C., and Cerdà, J. (2015). Gonadotropin-activated androgen-dependent and independent pathways regulate aquaporin expression during Teleost (*Sparus aurata*) spermatogenesis. *PLoS One* 10:e0142512. doi: 10.1371/journal.pone.0142512
- Bruce, A., Alexander, J., Julian, L., Martin, R., Keith, R., and Peter, W. (2002). *Molecular Biology of the Cell*, 4th Edn, New York, NY: Garland Science.
- Chauvigné, F., Fatsini, E., Duncan, N., Ollé, J., Zanuy, S., Gómez, A., et al. (2016). Plasma levels of follicle-stimulating and luteinizing hormones during the reproductive cycle of wild and cultured *Senegalese sole (Solea senegalensis)*. *Comp. Biochem. Physiol. Part A Mol. Integr. Physiol.* 191, 35–43. doi: 10.1016/j.cbpa.2015.09.015
- and Technology Innovation Project (No. 2018SDKJ0302-4), Shandong Province Key R&D Projects (No. 2019GHY112013), Natural Science Foundation of Shandong Province (No. ZR2018BC053), National Key Research and Development Program (No. 2018YFD0901204), Key Special Project for Introduced Talents Team of Southern Marine Science and Engineering Guangdong Laboratory (Guangzhou) (No. GML2019ZD0402), Major Agricultural Application Technology Innovation Project of Shandong Province (No. SD2019YY011), Qingdao National Laboratory for Marine Science and Technology (No. 2018SDKJ0502-2), China Agriculture Research System (No. CARS-47), Major Science and Technology for Scientific and Technological Innovation Projects (Shandong) (No. 2019JZZY020710), and STS Project (Nos. KFZD-SW-106, ZSSD-019, 2017T3017, and 2019T3022).
- Chauvigné, F., Parhi, J., Ollé, J., and Cerdà, J. (2017). Dual estrogenic regulation of the nuclear progesterin receptor and spermatogonial renewal during gilthead seabream (*Sparus aurata*) spermatogenesis. *Comp. Biochem. Physiol. Part A Mol. Integr. Physiol.* 206, 36–46. doi: 10.1016/j.cbpa.2017.01.008
- Chauvigné, F., Zapater, C., Crespo, D., Planas, J. V., and Cerdà, J. (2014a). Fsh and Lh direct conserved and specific pathways during flatfish semicystic spermatogenesis. *J. Mol. Endocrinol.* 53, 175–190. doi: 10.1530/JME-14-0087
- Chauvigné, F., Zapater, C., Gasol, J. M., and Cerdà, J. (2014b). Germ-line activation of the luteinizing hormone receptor directly drives spermiogenesis in a nonmammalian vertebrate. *Proc. Natl. Acad. Sci. U.S.A.* 111, 1427–1432. doi: 10.1073/pnas.1317838111
- Chen, S. X., Bogerd, J., Schoonen, N. E., Martijn, J., de Waal, P. P., and Schulz, R. W. (2013). A progesterin (17 $\alpha$ ,20 $\beta$ -dihydroxy-4-pregnen-3-one) stimulates early stages of spermatogenesis in zebrafish. *Gen. Comp. Endocrinol.* 185, 1–9. doi: 10.1016/j.ygcen.2013.01.005
- Chung, E. Y. (2008). Ultrastructure of germ cells, the Leydig cells, and Sertoli cells during spermatogenesis in *Boleophthalmus pectinirostris* (Teleostei, Perciformes, Gobiidae). *Tissue Cell.* 40, 195–205. doi: 10.1016/j.tice.2007.11.003
- Chung, E. Y., Yang, Y. C., Kang, H. W., Choi, K. H., Jun, J. C., and Lee, K. Y. (2010). Ultrastructure of germ cells and the functions of leydig cells and sertoli cells associated with spermatogenesis in *Pampus argenteus* (Teleostei: Perciformes: Stromateidae). *Zool. Stud.* 49, 39–50.
- Csaba, Z., Csernus, V., and Gerendai, I. (1998). Intratesticular serotonin affects steroidogenesis in the rat testis. *J. Neuroendocrinol.* 10, 371–376. doi: 10.1046/j.1365-2826.1998.00217.x
- da Cruz-Landim, C., Camargo Abdalla, F., and da Cruz-Höfling, M. A. (2003). Morphological study of the spermatogenesis in the teleost *Piaractus mesopotamicus*. *Biocell* 27, 319–328.

- de Waal, P. P., Wang, D. S., Nijenhuis, W. A., Schulz, R. W., and Bogerd, J. (2008). Functional characterization and expression analysis of the androgen receptor in zebrafish (*Danio rerio*) testis. *Reproduction* 136, 225–234. doi: 10.1530/REP-08-0055
- Díaz-Ramos, J., Flores-Flores, M., Ayala, M. E., and Aragón-Martínez, A. (2018). Impaired serotonin communication during juvenile development in rats diminishes adult sperm quality. *Syst. Biol. Reprod. Med.* 64, 340–347. doi: 10.1080/19396368.2018.1472825
- Dumasia, K., Kumar, A., Deshpande, S., Sonawane, S., and Balasinor, N. H. (2016). Differential roles of estrogen receptors, ESR1 and ESR2, in adult rat spermatogenesis. *Mol. Cell. Endocrinol.* 428, 89–100. doi: 10.1016/j.mce.2016.03.024
- Fallah-Rad, A. H., Connor, M. L., and Del Vecchio, R. P. (2001). Effect of transient early hyperthyroidism on onset of puberty in Suffolk ram lambs. *Reproduction* 121, 639–646. doi: 10.1530/rep.0.1210639
- FAO (2005). “Aquatic species information programme: *Psetta maxima*,” in *Aquatic Species Information Programme*, eds J. L. Rodríguez Villanueva and B. Fernández Souto (Rome: FAO Fisheries Division).
- Feng, C., Xu, S., Liu, Y., Wang, Y., Wang, W., Yang, J., et al. (2018). Progesterin is important for testicular development of male turbot (*Scophthalmus maximus*) during the annual reproductive cycle through functionally distinct progesterin receptors. *Fish. Physiol. Biochem.* 44, 35–48. doi: 10.1007/s10695-017-0411-y
- Fink, G., Sumner, B., Rosie, R., Wilson, H., and McQueen, J. (1999). Androgen actions on central serotonin neurotransmission: relevance for mood, mental state and memory. *Behav. Brain Res.* 105, 53–68. doi: 10.1016/s0166-4328(99)00082-0
- Frungieri, M. B., Zitta, K., Pignataro, O. P., Gonzalez-Calvar, S. I., and Calandra, R. S. (2002). Interactions between testicular serotonergic, catecholaminergic, and corticotropin-releasing hormone systems modulating cAMP and testosterone production in the golden hamster. *Neuroendocrinology* 76, 35–46. doi: 10.1159/000063682
- Gerendai, I., Banczerowski, P., Csernus, V., and Halász, B. (2007). Innervation and serotonergic receptors of the testis interact with local action of interleukin-1 beta on steroidogenesis. *Auton. Neurosci.* 131, 21–27. doi: 10.1016/j.autneu.2006.06.002
- Grandi, G., Astolfi, G., Chicca, M., and Pezzi, M. (2018). Ultrastructural investigations on spermatogenesis and spermatozoan morphology in the endangered Adriatic sturgeon, *Acipenser naccarii* (Chondrostei, Acipenseriformes). *J. Morphol.* 279, 1376–1396. doi: 10.1002/jmor.20847
- Greenbaum, M. P., Iwamori, T., Buchold, G. M., and Matzuk, M. M. (2011). Germ cell intercellular bridges. *Csh. Perspect. Biol.* 3:a005850. doi: 10.1101/cshperspect.a005850
- Gui, J., Tang, Q., Li, Z., Liu, J., and De Silva, S. S. (2018). *Aquaculture in China: Success Stories and Modern Trends*. Hoboken, NJ: Wiley-Blackwell.
- Hachero-Cruzado, I., Fornies, A., Herrera, M., Mancera, J. M., and Martínez-Rodríguez, G. (2013). Sperm production and quality in brill *Scophthalmus rhombus* L.: relation to circulating sex steroid levels. *Fish. Physiol. Biochem.* 39, 215–220. doi: 10.1007/s10695-012-9692-3
- Hermida, M., Bouza, C., Fernandez, C., Sciara, A. A., Rodríguez-Ramilo, S. T., Fernandez, J., et al. (2013). Compilation of mapping resources in turbot (*Scophthalmus maximus*): a new integrated consensus genetic map. *Aquaculture* 141, 19–25. doi: 10.1016/j.aquaculture.2013.07.040
- Hernandez, A. (2018). Thyroid hormone role and economy in the developing testis. *Vitam. Horm.* 106, 473–500. doi: 10.1016/bs.vh.2017.06.005
- Holsberger, D. R., Kiesewetter, S. E., and Cooke, P. S. (2005). Regulation of neonatal Sertoli cell development by thyroid hormone receptor alpha1. *Biol. Reprod.* 73, 396–403. doi: 10.1095/biolreprod.105.041426
- Huang, B., Wang, N., Wang, L., and Jia, Y. (2019). Vitamin E stimulates the expression of gonadotropin hormones in primary pituitary cells of turbot (*Scophthalmus maximus*). *Aquaculture* 509, 47–51. doi: 10.1016/j.aquaculture.2019.05.023
- Hyeon, J.-Y., Hur, S.-P., Kim, B.-H., Byun, J.-H., Kim, E.-S., Lim, B.-S., et al. (2019). Involvement of estrogen and its receptors in morphological changes in the eyes of the Japanese eel, *Anguilla japonica*, in the process of artificially-induced maturation. *Cells* 8:310. doi: 10.3390/cells8040310
- Kang, H.-W., Kim, S. H., and Chung, J. S. (2016). Ultrastructural studies of germ cell development and the functions of leydig cells and sertoli cells associated with spermatogenesis in *Kareius bicoloratus* (Teleostei, Pleuronectiformes, Pleuronectidae). *Dev. Reprod.* 20, 11–22. doi: 10.12717/DR.2016.20.1.011
- Kloas, W., Urbatzka, R., Opitz, R., Würtz, S., Behrends, T., Hermelink, B., et al. (2009). Endocrine disruption in aquatic vertebrates. *Ann. N. Y. Acad. Sci.* 1163, 187–200. doi: 10.1111/j.1749-6632.2009.04453.x
- Kreke, N., and Dietrich, D. R. (2008). Physiological endpoints for potential SSRI interactions in fish. *Crit. Rev. Toxicol.* 38, 215–247. doi: 10.1080/10408440801891057
- Kroll, M. M., Peck, M. A., Butts, I. A. E., and Trippel, E. A. (2013). Paternal effects on early life history traits in Northwest Atlantic cod, *Gadus morhua*. *J. Appl. Ichthyol.* 29, 623–629. doi: 10.1111/jai.12161
- Kumar, A., Dumasia, K., Deshpande, S., Raut, S., and Balasinor, N. H. (2018). Delineating the regulation of estrogen and androgen receptor expression by sex steroids during rat spermatogenesis. *J. Steroid. Biochem. Mol. Biol.* 182, 127–136. doi: 10.1016/j.jsbmb.2018.04.018
- Leal, M. C., Cardoso, E. R., Nóbrega, R. H., Batlouni, S. R., Bogerd, J., França, L. R., et al. (2009). Histological and stereological evaluation of zebrafish (*Danio rerio*) spermatogenesis with an emphasis on spermatogonial generations. *Biol. Reprod.* 81, 177–187. doi: 10.1095/biolreprod.109.076299
- Lehti, M. S., and Sironen, A. (2016). Formation and function of the manchette and flagellum during spermatogenesis. *Reproduction* 151, R43–R54. doi: 10.1530/REP-15-0310
- Lehti, M. S., and Sironen, A. (2017). Formation and function of sperm tail structures in association with sperm motility defects. *Biol. Reprod.* 97, 522–536. doi: 10.1093/biolre/i0x096
- Lei, J. (2003). The development direction of turbot farming industry in China. *Sci. Fish. Farm.* 7, 3–4.
- Lei, J. (2005). *The Theory and Technology of Marine Fish*. Beijing: Agriculture Press.
- Lei, J., and Men, Q. (2002). Lectures on artificial propagation and cultivation technology of Turbot (II). *Shandong. Fish.* 19, 43–46.
- Lin, F., Xu, S., Ma, D., Xiao, Z., Zhao, C., Xiao, Y., et al. (2012). Germ line specific expression of a vasa homologue gene in turbot (*Scophthalmus maximus*): evidence for vasa localization at cleavage furrows in *Euteleostei*. *Mol. Reprod. Dev.* 79, 803–813. doi: 10.1002/mrd.22120
- Lin, F., Zhao, C., Xu, S., Ma, D., Xiao, Z., Xiao, Y., et al. (2013). Germline-specific and sexually dimorphic expression of a dead end gene homologue in turbot (*Scophthalmus maximus*). *Theriogenology* 80, 665–672. doi: 10.1016/j.theriogenology.2013.06.016
- Lou, Y., and Takahashi, H. (1989). Spermiogenesis in the Nile tilapia *Oreochromis niloticus* with notes on a unique pattern of nuclear chromatin condensation. *J. Morphol.* 200, 321–330. doi: 10.1002/jmor.1052000307
- Luine, V. N., and Rhodes, J. C. (1983). Gonadal hormone regulation of MAO and other enzymes in hypothalamic areas. *Neuroendocrinology* 36, 235–241. doi: 10.1159/000123461
- Malison, J. A., Procarione, L. S., Barry, T. P., Kapuscinski, A. R., and Kayes, T. B. (1994). Endocrine and gonadal changes during the annual reproductive cycle of the freshwater teleost, *Stizostedion vitreum*. *Fish. Physiol. Biochem.* 13, 473–484. doi: 10.1007/BF00004330
- Maran, R. R., Arunakaran, J., and Aruldas, M. M. (2000). T3 directly stimulates basal and modulates LH induced testosterone and oestradiol production by rat Leydig cells in vitro. *Endocr. J.* 47, 417–428. doi: 10.1507/endocrj.47.417
- Martin, J. M., Bertram, M. G., Saari, M., Ecker, T. E., Hannington, S. L., Tanner, J. L., et al. (2019). Impact of the widespread pharmaceutical pollutant fluoxetine on behaviour and sperm traits in a freshwater fish. *Sci. Total. Environ.* 650, 1771–1778. doi: 10.1016/j.scitotenv.2018.09.294
- McDonald, M. D. (2017). An AOP analysis of selective serotonin reuptake inhibitors (SSRIs) for fish. *Comp. Biochem. Physiol. C Toxicol. Pharmacol.* 197, 19–31. doi: 10.1016/j.cbpc.2017.03.007
- Mendis-Handagama, S. M. L. C., and Siril Ariyaratne, H. B. (2005). Leydig cells, thyroid hormones and steroidogenesis. *Indian J. Exp. Biol.* 43, 939–962.
- Meston, C. M., and Gorzalka, B. B. (1992). Psychoactive drugs and human sexual behavior: the role of serotonergic activity. *J. Psychoact. Drugs* 24, 1–40. doi: 10.1080/02791072.1992.10471616
- Miciński, P., Pawlicki, K., Wielgus, E., Bochenek, M., Gogol, P., and Ficek, B. (2011). Total reactive antioxidant potential and DNA fragmentation index as fertility sperm parameters. *Reprod. Biol.* 11, 135–144. doi: 10.1016/s1642-431x(12)60050-3

- Miura, T., Higuchi, M., Ozaki, Y., Ohta, T., and Miura, C. (2006). Progesterin is an essential factor for the initiation of the meiosis in spermatogenic cells of the eel. *Proc. Natl. Acad. Sci. U.S.A.* 103, 7333–7338. doi: 10.1073/pnas.0508419103
- Miura, T., Yamauchi, K., Takahashi, H., and Nagahama, Y. (1992). The role of hormones in the acquisition of sperm motility in salmonid fish. *J. Exp. Zool.* 261, 359–363. doi: 10.1002/jez.1402610316
- Munakata, A., and Kobayashi, M. (2010). Endocrine control of sexual behavior in teleost fish. *Gen. Comp. Endocrinol.* 165, 456–468. doi: 10.1016/j.ygcen.2009.04.011
- Mylonas, C. C., Fostier, A., and Zanuy, S. (2010). Broodstock management and hormonal manipulations of fish reproduction. *Gen. Comp. Endocrinol.* 165, 516–534. doi: 10.1016/j.ygcen.2009.03.007
- O'Shaughnessy, P. J. (2014). Hormonal control of germ cell development and spermatogenesis. *Semin. Cell. Dev. Biol.* 29, 55–65. doi: 10.1016/j.semcdb.2014.02.010
- Palma, P., Takemura, A., Libunao, G. X., Superio, J., de Jesus-Ayson, E. G., Ayson, F., et al. (2019). Reproductive development of the threatened giant grouper *Epinephelus lanceolatus*. *Aquaculture* 509, 1–7. doi: 10.1016/j.aquaculture.2019.05.001
- Ribas, L., Robledo, D., Gómez-Tato, A., Viñas, A., Martínez, P., and Piferrer, F. (2017). Transcriptomic study of gonadal sex differentiation in turbot (*Scophthalmus maximus*) using a species-specific microarray enriched with reproduction-related genes. *Aquaculture* 472:167. doi: 10.1016/j.aquaculture.2017.03.032
- Rupik, W., Huszno, J., and Klag, J. (2011). Cellular organisation of the mature testes and stages of spermiogenesis in *Danio rerio* (Cyprinidae; Teleostei) - structural and ultrastructural studies. *Micron* 42, 833–839. doi: 10.1016/j.micron.2011.05.006
- Safarinejad, M. R. (2008). Sperm DNA damage and semen quality impairment after treatment with selective serotonin reuptake inhibitors detected using semen analysis and sperm chromatin structure assay. *J. Urol.* 180, 2124–2128. doi: 10.1016/j.juro.2008.07.034
- Schulz, R. W., de França, L. R., Lareyre, J.-J., Le Gac, F., LeGac, F., Chiarini-Garcia, H., et al. (2010). Spermatogenesis in fish. *Gen. Comp. Endocrinol.* 165, 390–411. doi: 10.1016/j.ygcen.2009.02.013
- Schulz, R. W., Liemburg, M., García-López, A., Dijk, W. V., and Bogerd, J. (2008). Androgens modulate testicular androgen production in African catfish (*Clarias gariepinus*) depending on the stage of maturity and type of androgen. *Gen. Comp. Endocrinol.* 156, 154–163. doi: 10.1016/j.ygcen.2008.01.002
- Scott, A. P., Sumpter, J. P., and Stacey, N. (2010). The role of the maturation-inducing steroid, 17,20beta-dihydroxypregn-4-en-3-one, in male fishes: a review. *J. Fish. Biol.* 76, 183–224. doi: 10.1111/j.1095-8649.2009.02483.x
- Siddique, M. A., Linhart, O., Krejszef, S., Žarski, D., Pitcher, T. E., Politis, S. N., et al. (2017). Paternal identity impacts embryonic development for two species of freshwater fish. *Gen. Comp. Endocrinol.* 1, 30–35. doi: 10.1016/j.ygcen.2016.07.004
- Song, Z., Wang, X., Xue, R., Xiao, Z., Ma, D., Liu, Q., et al. (2019). Study on characteristics of post-ovulation aging in ovarian cavity of turbot. *Mar. Sci.* 43, 106–111. doi: 10.11759/hyxx20190314002
- Takeshi, M., and Chiemi, M. (2003). Molecular control mechanisms of fish spermatogenesis. *Fish. Physiol. Biochem.* 28, 181–186. doi: 10.1023/B:FISH.0000030522.71779.47
- Tang, E. I., Mruk, D. D., and Cheng, C. Y. (2016). Regulation of microtubule (MT)-based cytoskeleton in the seminiferous epithelium during spermatogenesis. *Semin. Cell. Dev. Biol.* 59, 35–45. doi: 10.1016/j.semcdb.2016.01.004
- Taranger, G. L., Carrillo, M., Schulz, R. W., Fontaine, P., Zanuy, S., Felip, A., et al. (2010). Control of puberty in farmed fish. *Gen. Comp. Endocrinol.* 165, 483–515. doi: 10.1016/j.ygcen.2009.05.004
- Tubbs, C., and Thomas, P. (2008). Functional characteristics of membrane progesterin receptor alpha (mPRalpha) subtypes: a review with new data showing mPRalpha expression in seatrout sperm and its association with sperm motility. *Steroids* 73, 935–941. doi: 10.1016/j.steroids.2007.12.022
- Tyminski, J. P., Gelslechter, J. J., and Motta, P. J. (2015). Androgen receptors in the bonnethead, *Sphyrna tiburo*: cDNA cloning and tissue-specific expression in the male reproductive tract. *Gen. Comp. Endocrinol.* 224, 235–246. doi: 10.1016/j.ygcen.2015.08.018
- Ueda, H., Kambegawa, A., and Nagahama, Y. (1985). Involvement of gonadotrophin and steroid hormones in spermiation in the amago salmon, *Oncorhynchus rhodurus*, and goldfish, *Carassius auratus*. *Gen. Comp. Endocrinol.* 59, 24–30. doi: 10.1016/0016-6480(85)90415-0
- Ventelä, S., Toppari, J., and Parvinen, M. (2003). Intercellular organelle traffic through cytoplasmic bridges in early spermatids of the rat: mechanisms of haploid gene product sharing. *Mol. Biol. Cell.* 14, 2768–2780. doi: 10.1091/mbc.e02-10-0647
- Wagner, M. S., Wajner, S. M., and Maia, A. L. (2008). The role of thyroid hormone in testicular development and function. *J. Endocrinol.* 199, 351–365. doi: 10.1677/JOE-08-0218
- Walters, K. A., Simanainen, U., and Handelsman, D. J. (2010). Molecular insights into androgen actions in male and female reproductive function from androgen receptor knockout models. *Hum. Reprod. Update* 16, 543–558. doi: 10.1093/humupd/dmq003
- Wang, X., Liu, Q., Xu, S., Xiao, Y., Wang, Y., Feng, C., et al. (2018). Transcriptome dynamics during turbot spermatogenesis predicting the potential key genes regulating male germ cell proliferation and maturation. *Sci. Rep.* 8:15825. doi: 10.1038/s41598-018-34149-5
- Weltzien, F.-A., Andersson, E., Andersen, O., Shalchian-Tabrizi, K., and Norberg, B. (2004). The brain-pituitary-gonad axis in male teleosts, with special emphasis on flatfish (*Pleuronectiformes*). *Comp. Biochem. Physiol. A Mol. Integr. Physiol.* 137, 447–477. doi: 10.1016/j.cbpb.2003.11.007
- Weltzien, F.-A., Taranger, G. L., Karlsen, Ø., and Norberg, B. (2002). Spermatogenesis and related plasma androgen levels in Atlantic halibut (*Hippoglossus hippoglossus* L.). *Comp. Biochem. Physiol. A Mol. Integr. Physiol.* 132, 567–575. doi: 10.1016/s1095-6433(02)00092-2
- Zhang, X., Wang, W., Xiao, Z., Xu, C., Jiang, R., Xu, S., et al. (2013). Physiological characteristics and ultrastructure of post-thaw sperm in turbot *scophthalmus maximus*. *Oceanol. Limnol. Sinica* 44, 1103–1107.
- Zhao, C., Xu, S., Feng, C., Liu, Y., Yang, Y., Wang, Y., et al. (2018). Characterization and differential expression of three GnRH forms during reproductive development in cultured turbot *Scophthalmus maximus*. *J. Ocean. Limnol.* 36, 1360–1373. doi: 10.1007/s00343-018-7068-y
- Zhao, C., Xu, S., Liu, Y., Wang, Y., Liu, Q., and Li, J. (2017). Gonadogenesis analysis and sex differentiation in cultured turbot (*Scophthalmus maximus*). *Fish. Physiol. Biochem.* 43, 265–278. doi: 10.1007/s10695-016-0284-5
- Zhou, L., Wang, X., Liu, Q., Xu, S., Zhao, H., Han, M., et al. (2019). Visualization of turbot (*Scophthalmus maximus*) primordial germ cells in vivo using fluorescent protein mediated by the 3' untranslated region of *nanos3* or *vasa* gene. *Mar. Biotechnol.* 21, 671–682. doi: 10.1007/s10126-019-09911-z

**Conflict of Interest:** ZS was employed by the company Weihai Shenghang Aquatic Product Science and Technology Co. Ltd.

The remaining authors declare that the research was conducted in the absence of any commercial or financial relationships that could be construed as a potential conflict of interest.

Copyright © 2021 Liu, Liu, Xu, Wang, Feng, Zhao, Song and Li. This is an open-access article distributed under the terms of the Creative Commons Attribution License (CC BY). The use, distribution or reproduction in other forums is permitted, provided the original author(s) and the copyright owner(s) are credited and that the original publication in this journal is cited, in accordance with accepted academic practice. No use, distribution or reproduction is permitted which does not comply with these terms.